TECHNICAL MEMORANDUM

492

Use of Analysis Ensembles in Estimating Flow-Dependent Background Error Variances

Ersin Kucukkaraca
and Michael Fisher

Research Department

April 2006

European Centre for Medium-Range Weather Forecasts
Europäisches Zentrum für mittelfristige Wettervorhersage
Centre européen pour les prévisions météorologiques à moyen

Series: ECMWF Technical Memoranda

A full list of ECMWF Publications can be found on our web site under:
http://www.ecmwf.int/publications/

Contact: library@ecmwf.int

Summary

This paper represents a preliminary investigation into the use of ensembles of analyses to estimate flow-dependent variances of background error. We study small-scale, dynamically-active systems in the mid latitudes (the storms over France during 26-28th December 1999) and in the tropics (Hurricane Isabel, 6-29th September 2003). We demonstrate that the use of ensemble-based estimates of background error variance can improve the analysis of such systems. Although the approach has considerable potential, we note that good analyses of such small-scale systems are unlikely to be produced unless they are adequately resolved both by the main analysis system, and by the members of the analysis ensemble. We believe that a small ensemble of relatively high resolution members may be preferable to a larger ensemble of lower resolution members. We also highlight the tendency of the analysis ensemble to under-estimate the variance of analysis and background error, particularly in dynamically inactive regions. We consider a few simple measures that try to correct this under-estimate, but note that a better understanding (and representation) of the effects of model error, and of the spatial and inter-channel correlation of observation error, is needed before such *ad hoc* measures can be eliminated.

1. Introduction

Data assimilation for Numerical Weather Prediction (NWP) blends observations with *a priori* (background) information from a short-range forecast to produce an analysis of the current state of the atmosphere. The success of this blending, which is crucial to the accuracy of the subsequent forecast, depends on the provision of good estimates of the statistical properties of the observation and background errors.

In this paper, we consider one component of these error statistics: the variances of background error. These are difficult to determine, since we do not have knowledge of the true state of the atmosphere. They are frequently estimated from surrogate quantities with statistical and dynamic properties assumed similar to those of the unknown errors (e.g. Parrish and Derber, 1992). The properties are built into the background-error covariance matrix for data assimilation, the purpose of which is to spread observed information to nearby grid points and levels and to other variables.

In the current ECMWF analysis system, variances of background errors are estimated using the method proposed by Fisher and Courtier (1995), and implemented operationally in 1996. The method may be divided into three stages. First, a randomization technique is used to diagnose the variances of background error in effect for the current cycle. This step is necessary because the variances for some variables are not directly specified, but are defined implicitly through the action of linear operators (describing balance, radiative transfer, etc.) on the specified background error covariance matrix. Next, the variances are reduced to produce an estimate of the variances of analysis error. The reduction is determined as a function of the leading eigenvectors of the Hessian matrix of the analysis cost function. Finally, a simple error-growth model (Savijärvi, 1995) is applied in order to account for the growth in error during the forecast. The result is an estimate of error variance for the short-term forecast that provides the background for the next cycle of analysis. The method is repeated at each analysis cycle.

The current method for estimating background error variance incorporates a degree of flow-dependence. This arises from the use of balance operators that depend on the background state, and because the eigenvectors of the 4D-Var Hessian incorporate a knowledge of the dynamical evolution during the analysis window. However, the error-growth model that propagates errors from cycle to cycle is extremely simple, and does not take into account the nature of the flow. As a consequence, current background errors are largely a function of data density, with a fairly weak dependence on the underlying flow.

A further shortcoming of the current approach arises from the use of a truncated eigenvector expansion to determine the difference between background error and analysis error. This results in an over-estimate of the variance of analysis error. Moreover, since the leading eigenvectors correspond to the best observed features, the best estimates of analysis error variance occur in well-observed regions and for well-observed variables, whereas the variance in poorly-observed regions and for poorly-observed variables may be significantly over-estimated.

In this paper we investigate an alternative method for estimating the variances of analysis and background error. In this approach, an ensemble of analyses is run in parallel with the main analysis/forecast system. Each member of the ensemble is perturbed in such a way that the spread of the ensemble provides an estimate of the required variance. This approach to determining background error statistics is fundamental to the ensemble Kalman filter (Houtekamer and Mitchell, 1998; Evensen, 2003). However, unlike the ensemble Kalman filter, we do not attempt to determine the correlation structure of background error from the ensemble, but restrict ourselves to estimating their variance.

The rest of the paper is divided into four main sections. Section 2 describes the use of data assimilation ensembles to estimate background errors. In section 3, we discuss experiments for the 'French Storm' cases, 26-28th December 1999. Section 4 presents results for the tropical cyclone 'Hurricane Isabel' cases, 6-29th September 2003. We present some tentative conclusions in the final section.

2. Methodology

Suppose we add random perturbations to the background, observations and sea surface temperature (SST) of the analysis system. The result will be a perturbed analysis. Suppose now that a short forecast is run from the perturbed analysis, such as is required to produce the background field for the next analysis cycle. The result will be a perturbed forecast. Furthermore, provided the input perturbations have the appropriate statistical characteristics (and neglecting the effects of model error), the perturbation to the forecast will have the statistical characteristics of short-term forecast (background) error.

If we run a new cycle of analysis with perturbed inputs, we may use the perturbed forecast to provide the analysis with perturbed background fields. This allows a second perturbed analysis and forecast to be produced without requiring us explicitly to specify new perturbations to the background. This process may be continued for many analysis cycles. Furthermore, after a few days, the statistical characteristics of the perturbations of the analysis and forecast fields will depend only weakly on the initial background perturbation, so that a sequence of background fields may be generated whose statistical characteristics are essentially independent of the initial background perturbation (Fisher, 2003).

If we run the perturbed analysis-forecast system several times for the same period, with different random perturbations, we may generate an ensemble of perturbed members. Differences between the background fields of ensemble members provide surrogates for samples of background error (Fisher, 2003).

The method is illustrated schematically in Figure 1, in which time is running from left to right, and each row represent an independent, cycling 4D-Var analysis ensemble member. The blown-up portion of the figure (in the dashed box) shows that each input of the analysis is perturbed: the background x^b, the observation vector y and the surface fields (here represented by *SST*), with errors ε^b, ε^o and ε^{SST}, respectively. Provided the perturbations are drawn from distributions with the true random errors of the inputs, then the output perturbations will have the statistical characteristics of analysis error (ε^a) and forecast error (ε^f). The input perturbations for each member of the analysis ensemble are provided by independent random draws from the appropriate distribution. For each analysis cycle, and at each grid point, we calculate the standard deviation of background error as the ensemble spread, among the all members, of the short-range forecasts that provide the background fields for the next analysis cycle. This estimate of background error is used in a separate, unperturbed analysis, indicated by the two boxes at the bottom of Figure 1. In the experiments presented here, the unperturbed analysis was run at a higher horizontal resolution than the ensemble members.

A description of the method we used to perturb the observations was presented by Žagar at al. (2005). For most observations, we applied independent Gaussian perturbations with zero mean and variance equal to the prescribed variance of observation error. Spatially correlated perturbations were applied to Atmospheric Motion Vectors (AMVs), according to the model of Bormann et al. (2003).

The sea surface temperature used in the ECMWF analysis system is taken from an independent analysis (Thiebaux et al. 2001). Since it is an input to the analysis system, it must be perturbed in the ensemble members according to its assumed error characteristics. For this purpose, we used Vialard et al.'s (2005) estimate of random error in the sea surface temperature analysis. No perturbations were applied to surface fields over land.

In principle, the effect of model error could be represented as a stochastic forcing of the model. However, the statistical characteristics of model error are very poorly known, and we chose not to force the model in this way. We comment later that this may contribute to a lack of spread of the ensemble, particularly in dynamically inactive regions.

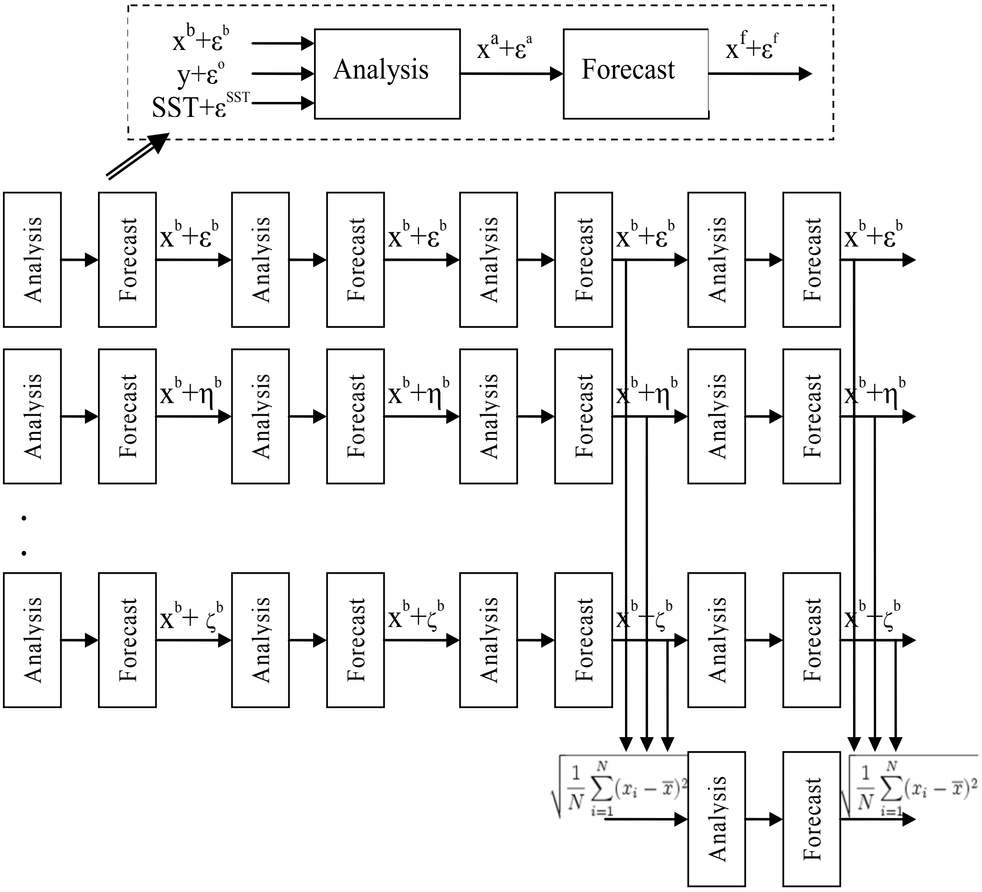

Figure 1: Schematic illustration of the analysis-ensemble method. Estimates of the standard deviations of analysis and short-range forecast error are shown as $\sqrt{\frac{1}{N}\sum_{i=1}^{N}\left(x_i-\bar{x}\right)^2}$ *, and provide input to the main analysis, represented by the bottom two boxes.*

3. French Storms

Two storms hit central Europe with unprecedented violence on 26th and 27th December 1999. In Southern Germany, Switzerland, Austria, and particularly in France, these Storms caused more than 100 deaths, felled over 270 million trees, and caused damage amounting to billions of US dollars (Bell et al. 2000). The atmospheric flow during this period was very complex, with small-scale vortices developing and interacting while moving very rapidly in a strong zonal flow. Global forecasts issued on successive days showed strong inconsistencies, confirming the difficulty for prediction of this episode (Buizza and Hollingsworth, 2002).

The First “French Storm” (26th December 1999) was small-scale and moved very rapidly. An initially weak low pressure system moved across the North Atlantic on 25th December while moderately deepening. At 0000 UTC on 26th December it was situated off the Brittany coast, with a central pressure of 980 hPa. Over the following six hours this low pressure system deepened rapidly by 20 hPa and reached the mouth of the Seine River at 0600 UTC. This rapid deepening was mainly caused by the interaction of the low pressure system with the left exit region of an exceptionally strong jet in the upper troposphere, which was characterized by strong divergence in the upper troposphere and positive vorticity advection at mid-levels (Wernli et al. 2002).

The Second Storm (27th December 1999) was larger in scale than the first. It produced winds which reached 150 km/h and spread a trail of destruction along the north coast of Spain, in south-west France and across many countries bordering the Mediterranean Sea. This storm killed 12 people in France, and a further 5 in Spain. Electricity supplies to a million homes were disrupted.

3.1 Description of the experiments

For this study we applied the analysis-ensemble method described in section 2 using two ensembles of different sizes. For the first experiment, background errors were obtained from a 5-member ensemble. For the second experiment, we used a 10 member ensemble. Each member of the analysis ensemble was run for the period 12th to 30th December 1999 using version CY29R1 of ECMWF's Integrated Forecast System (IFS) and T255, L60 resolution. The analysis method was 4D-Var with a 12-hour analysis window.

Figure 2a shows the standard deviation of 12-hour forecast error for geopotential height at 500hPa for 2100 UTC 26th December 1999, diagnosed from the 10-member ensemble. Maximum errors are located over the Atlantic, in the region corresponding to the area of cyclogenesis (the second "French Storm"). The maximum value is 3.7m, and the smallest errors (0.1m) are over the North Sea.

These estimates are small compared with the estimates provided by the method used in the current operational system (Figure 2d). Although the latter are unlikely to be particularly accurate, and certainly show no obvious dynamical features, it seems clear that the ensemble method severely under-estimates the magnitude of background error in this case. For this reason, an inflation factor of two was applied to the standard deviations. The resulting background errors are shown in Figure 2b. However, whereas inflating the background errors increases them significantly over the dynamically active region, estimated errors over the North Sea remain locally below 0.5m. It seems that a constant scaling factor is not enough to increase errors to realistic values in regions of very small spread. We believe that this under-estimation of forecast error variance in dynamically inactive regions may, in part, be a consequence of the lack of any representation of the effects of model error in our ensemble. In addition, there are sources of error that are common to all ensemble members (due to inappropriate error correlations, mis-specification of observation error variances, etc.). These do not contribute to the spread of the ensemble, but nevertheless contribute to analysis and forecast error.

To address the lack of ensemble spread in dynamically inactive regions, we devised a hybrid method whereby the background error variance was computed using the relationship

$$\sigma_b^2 = \max\left(\beta_1\sigma_1^2\,,\beta_2\sigma_2^2\right) \tag{1}$$

Here, σ_1^2 is the background error variance obtained from analysis ensemble members (as described in section 2), and σ_2^2 is the variance provided by the current operational method. The parameters β_i are fixed weights. The function attempts to use the flow-dependent estimate of background error provided by the ensemble in dynamically active regions, but uses the static estimate in relatively inactive regions, where the ensemble has very little spread. Figure 2c shows the hybrid background error estimate for $\beta_1 = 2, \quad \beta_2 = 0.5$.

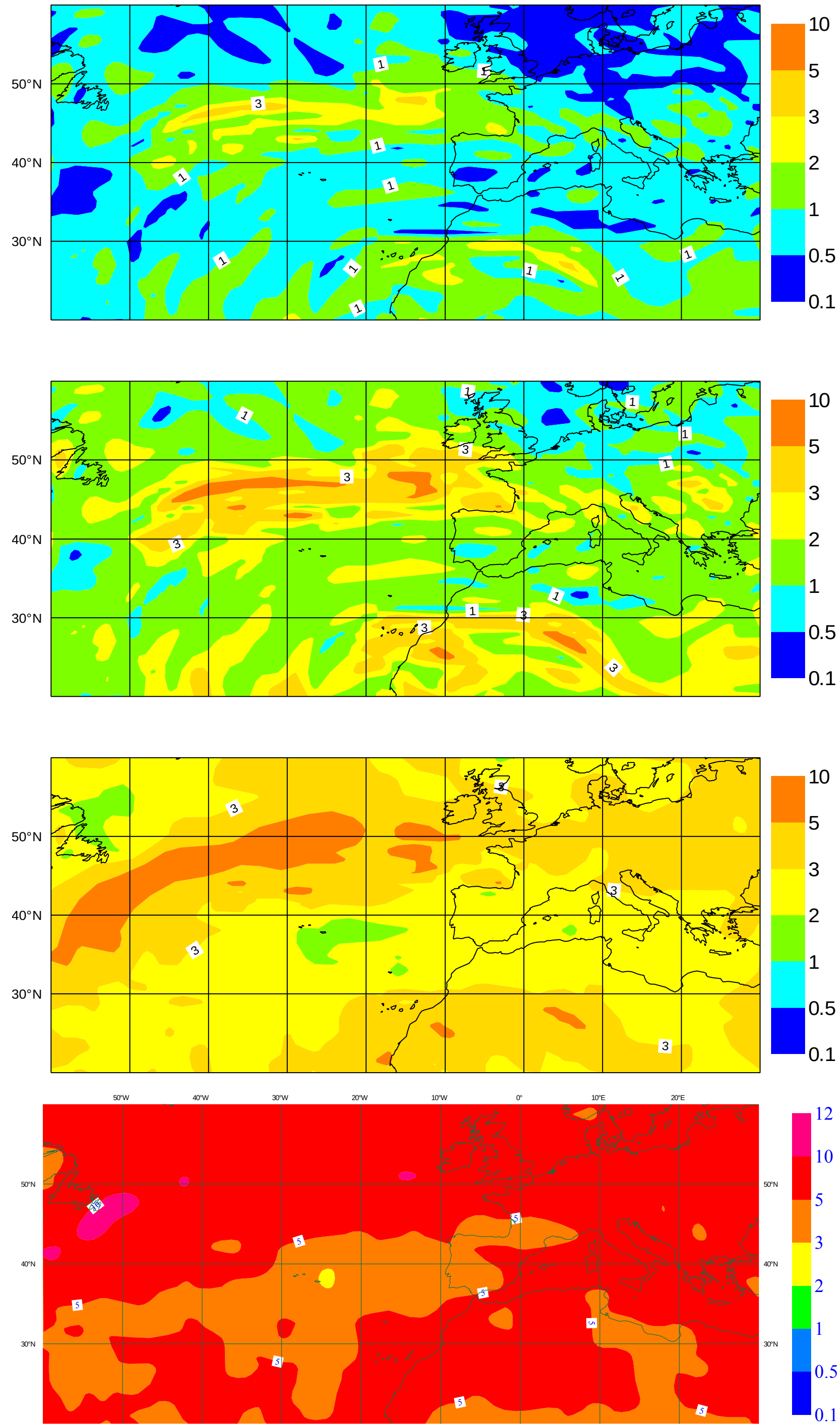

Figure 2: 12h forecast errors of geopotential height (m), 26th December 1999, 2100 UTC. Errors are shown for model level 39 (approximately 500 hPa). Panel (a) shows the errors obtained from a 10-member T255 ensemble of data assimilation . Panel (b) shows the same errors, inflated by a factor of 2. A hybrid estimate of background error (see text for details) is shown in panel (c), and errors calculated using the current operational method are shown in panel (d).

Experiments were run to assess the impact on the analysis system of replacing the standard deviations of background error with estimates derived from the analysis ensembles. These estimates were used both in the quality control (first-guess check) and in the definition of the background cost function. All these experiments were run using 4D-Var at a resolution of T511/T159 for the period 17th to 30th December 1999. Note that the initial date for these experiments is five days later than the initial date of the ensembles. This is to allow the ensemble members time to spread out from their identical initial conditions. The experiments are summarised in Table 1.

Control	Errors obtained using the current operational method.
anENS/5	Errors obtained from a 5-member ensemble.
anENS/5/2x	Errors obtained from a 5-member ensemble, and inflated by a factor of 2.
anENS/10	Errors obtained from a 10-member ensemble.
anENS/10/2x	Errors obtained from a 10-member ensemble, and inflated by a factor of 2.
anENS/Hyb	Errors obtained using the hybrid method from a 10-member ensemble.

Table 1: Analysis Experiments for the French Storms.

Figure 3a shows the geopotential height and wind at 1000hPa from the control experiment for 0600 UTC on 27th December 1999. The other panels in Figure 3 show estimates of 12-hour forecast error for wind speed on model level 57 (approximately 1000hPa) at 0900 UTC.

Figure 3b shows the background error of wind speed for the control experiment. Errors are between 2 and 3 m/s over the Atlantic and 1 to 2 m/s over the North Sea and much of Europe. There is no obvious connection between the errors and the underlying dynamical situation. By contrast, errors derived from the analysis ensembles (panels c to f) show a clear maximum associated with the developing low-pressure system.

Figure 3c (anENS/5/2x) shows the standard deviation of 12-hour forecast error, obtained from the 5-member ensemble and scaled by a factor of two. The corresponding un-scaled standard deviations are shown in Figure 3d. The small size of the 5-member ensemble results in some noise in the estimated standard deviations. This noise is reduced in the estimates derived from the 10-member ensemble, as shown by Figure 3e (anENS/10/2x).

The hybrid background error estimate (Figure 3f) is identical to the corresponding ensemble estimate (Figure 3e) over most of the Atlantic, where background errors in the control experiment are assumed to be small. Over land, the regions of unrealistically small errors have been eliminated.

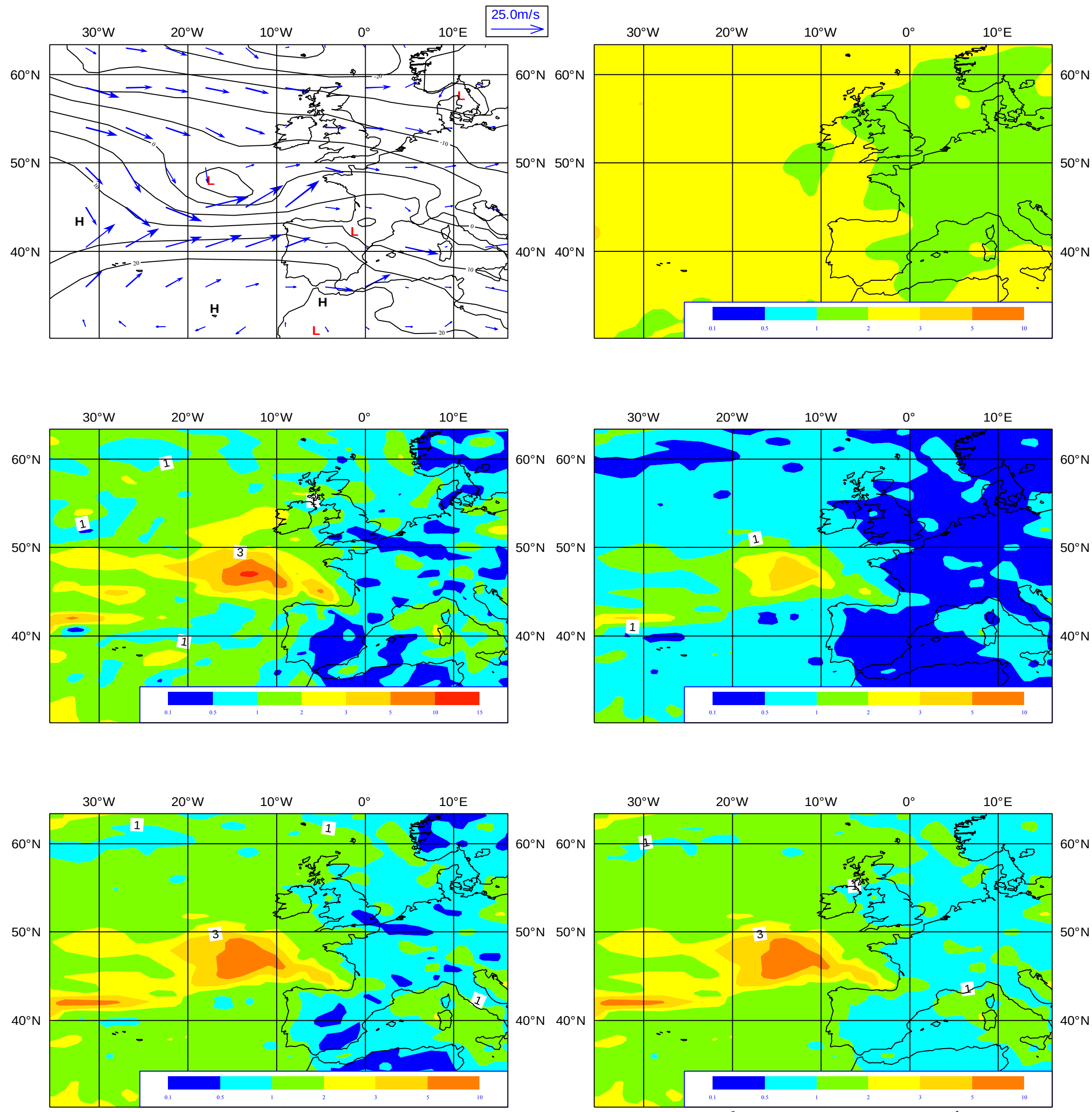

Figure 3: Panel (a): 1000 hPa analysis of height (dm) and wind (ms^{-1}) at 0600 UTC on 27th December 1999. The contour interval is 5 dm. The remaining panels show estimates of 12-Hour ensemble-based forecast errors of wind speed (ms^{-1}) for 26th December 1999, 2100 UTC, t+12 at model level 57 (approximately 1000 hPa). Panel (b): control run; (c) anENS/5/2x; (d) anENS/5; (e) anENS/10/2x; (f) anENS/hyb.

3.2 Performance of Analysis-Ensemble

Figure 4 shows the MSLP analyses at 1200 UTC on 26th December (the first "French Storm") for the experiments defined in Table 1. The low pressure system is located over Germany. All experiments produced very similar analyses in terms of location and central pressure. For anENS/5 (Figure 4b) the central pressure is 0.4 hPa deeper than for the control run (Figure 4a). The experiment using a hybrid error estimate (ansEN/hyb) produced a low 0.6hPa weaker than the control (Figure 4f).

The next analysis cycle (0000 UTC on 27th December, not shown) still showed little difference between the six MSLP analyses. However, at the following cycle (1200 UTC on 27th December), all the experiments that used ensemble-derived errors performed better than the control run. The central pressures of the main cyclone (the second “French Storm”) in these analyses (Figure 5b-f) were between 6.3 and 8.2 hPa deeper than control analysis (Figure 5a), which was too weak. The analysis produced using hybrid background errors (anENS/hyb, Figure 5f) had a higher central pressure than any of the experiments whose background errors were derived solely from an ensemble, but was still considerably lower than the control. However, this experiment also rejected fewer observations. For example, of the 1179 synoptic observation on the map area (36^{o}N/16^{o}W/62.5^{o}N/18^{o}E) between 0009 and 1500 UTC on 27th December, the control run, anENS/10/2x and anENS/hyb used respectively 1076, 1057 and 1075 observations. (Note that in the case of anENS/10/2x, many of the rejections occured in regions with little dynamic activity, where the ensemble method produced unrealistically low estimates of forecast error variance, as discussed in section 3.1.)

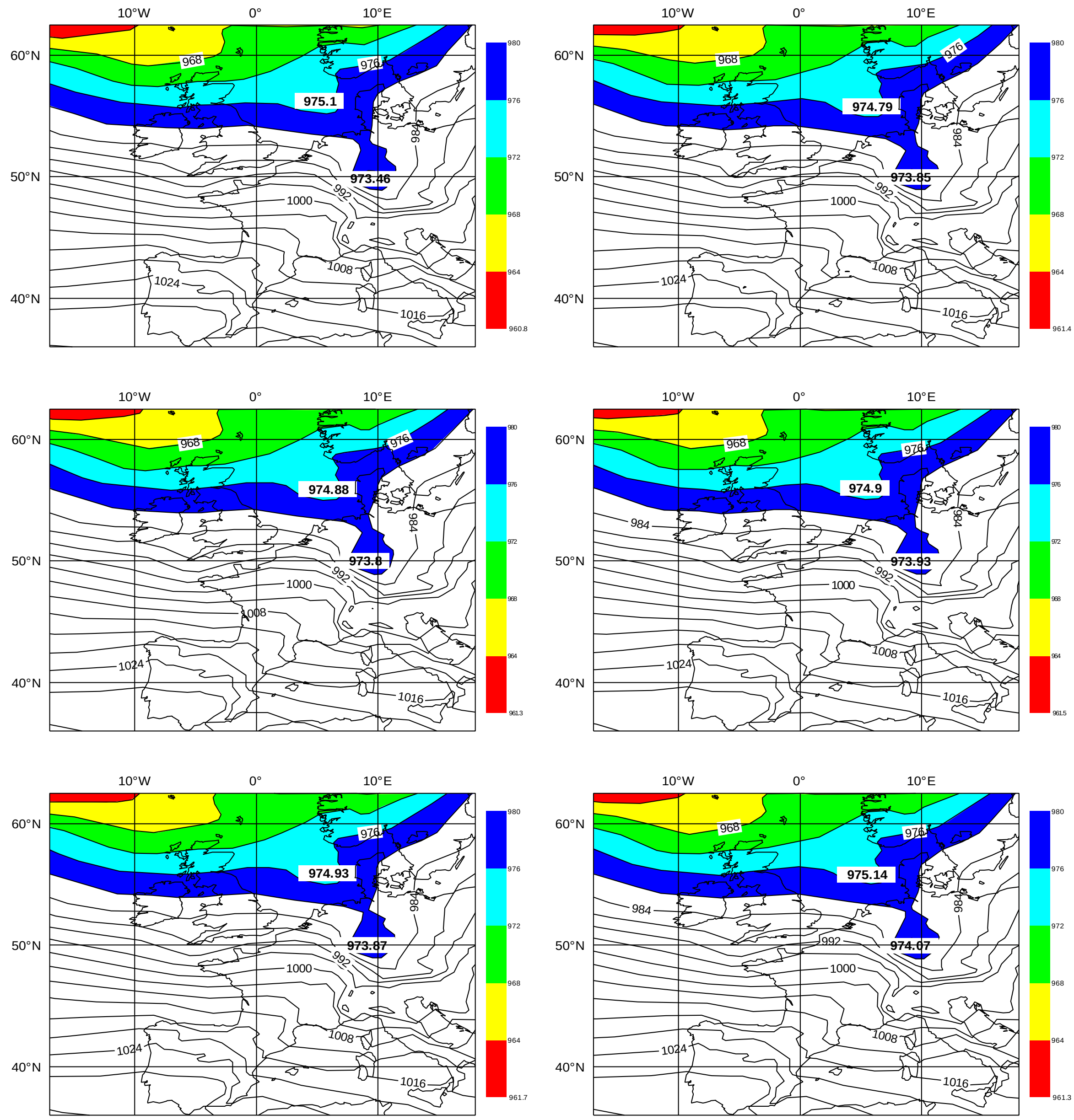

Figure 4: First French Storm MSLP analysis at 1200 UTC on 26th December 1999. Panel (a) shows the control, (b) shows experiment anENS/5, (c) shows enENS/5/2x, (d) shows anENS/10, (e) shows anENS/10/2x, and (f) shows anENS/hyb. The contour interval is 4 hPa, with shading for values below 980 hPa.

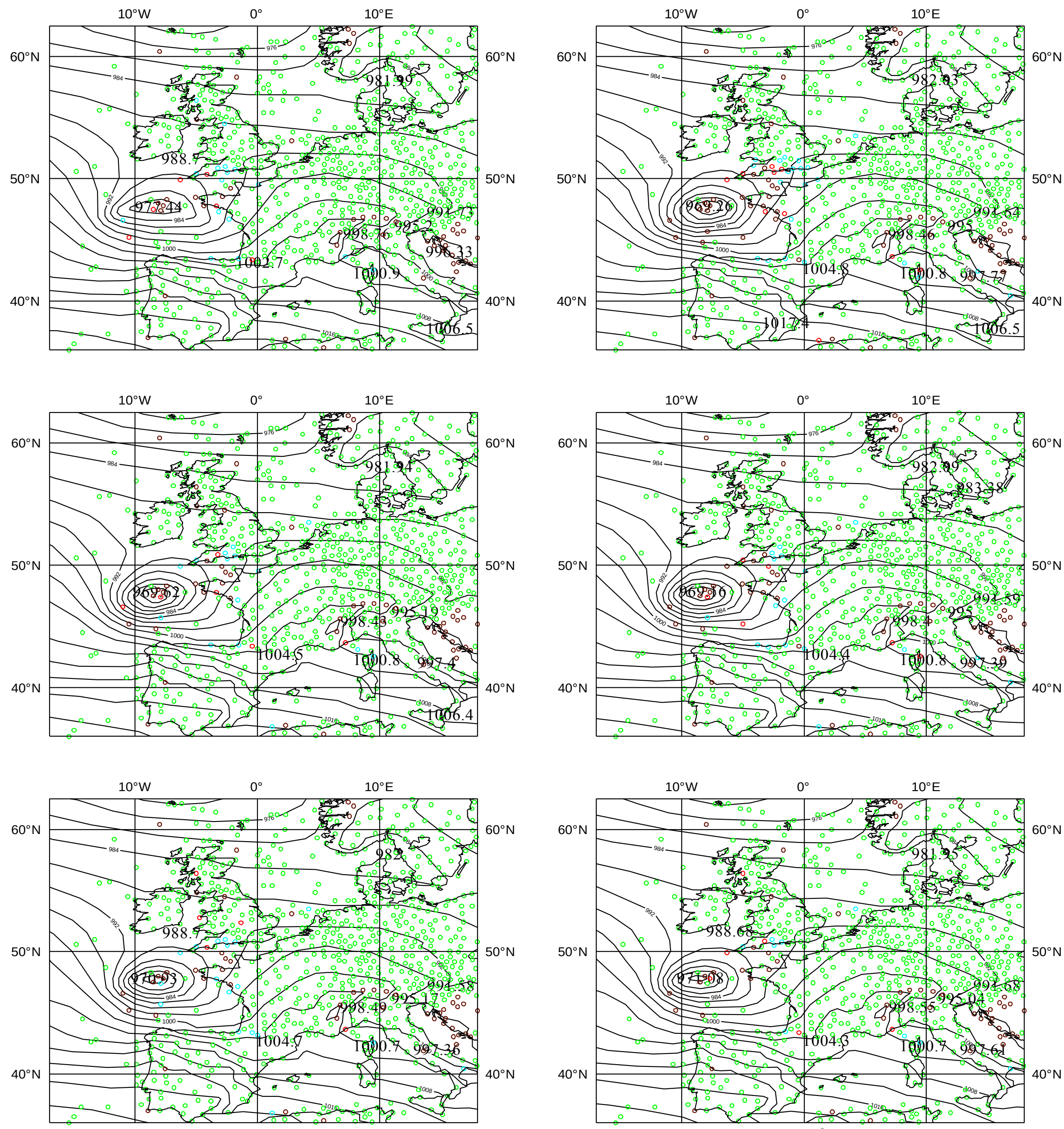

Figure 5: MSLP analyses for the second "French Storm" at 1200 UTC on 27th December 1999. The ordering of the panels is the same as in Figure 4. The contour interval is 4 hPa. Observations used by the analysis are shown by green symbols, whereas red symbols show obsevations that were rejected by quality control. The central pressures of the low pressure system in the six panels are as follows: (a) control 977.44hPa; (b) anENS/5 969.26hPa; (c) anENS/5/2x 969.62hPa; (d) anENS/10 969.16hPa; (e) anENS/10/2x 970.03hPa; (f) anENS/hyb 971.08hPa.

4. Tropical Cyclone Case

In this section, we discuss the performance of the analysis-ensemble system for Hurricane Isabel (September 2003): a long-lived Cape Verde hurricane that reached Category 5 status on the Saffir-Simpson Hurricane Scale (Simpson and Riehl 1981). Isabel is considered to be one of the most significant tropical cyclones to affect portions of north-eastern North Carolina and east-central Virginia since Hurricane Hazel in 1954 and the Chesapeake-Potomac Hurricane of 1933 (Beven and Cobb, 2004).

Isabel formed from a tropical wave that moved westward from the coast of Africa on 1 September. Over the next several days, the wave moved slowly westward and gradually became better organized. By 0000 UTC on 5 September, there was sufficient organized convection for satellite-based Dvorak intensity estimates to begin (Dvorak, 1975). Development continued, and it is estimated that a tropical depression formed at 0000 UTC on 6 September, with the depression becoming Tropical Storm Isabel six hours later, and a category 1 hurricane by 1500 UTC on 7 September. Isabel continued to increase in intensity, and became a category 5 hurricane at 2100 UTC on 11 September.

Increased vertical wind shear on 15 September caused Isabel to gradually weaken. The system weakened below major hurricane status (96 kt, or Category 3 on the Saffir-Simpson Hurricane Scale) on 16 September. It maintained Category 2 status with 85-90 kt maximum winds for the next two days while the overall size of the hurricane increased. Isabel made landfall near Drum Inlet, North Carolina at 1700 UTC 18 September, as a Category 2 hurricane (Beven and Cobb, 2004).

4.1 Performance of Analysis-Ensemble

For this case, we used a 10-member analysis ensemble. Each member was run for the period 1 September to 7 October 2003 with IFS cycle CY29R1 and a T255/T159, L60, 4D-Var analysis system.. In addition to the analysis ensemble, we ran two T511/T155 L60 4D-Var experiments for the period 6 September to 5 October 2003. The first (control) experiment used the operational method to calculate background errors. The second (ENSx2) used background errors calculated from the ensemble spread, and inflated by a factor of two.

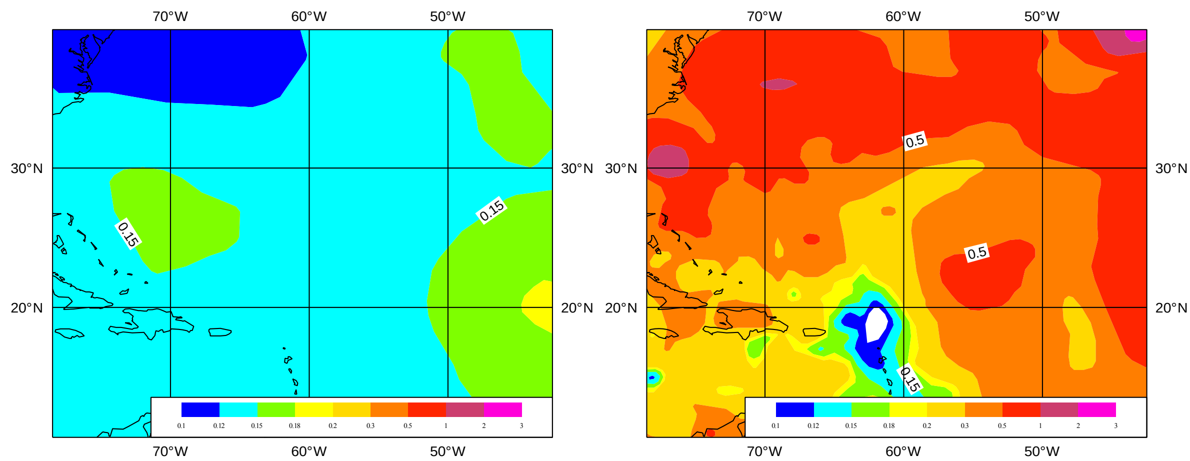

Figure 6: Background error of sea level pressure (hPa), 2100 UTC 11th September 2003. The left panel is for the control run, the right is obtained from the analysis ensemble (scaled by a factor of two).

Figure 6 shows the background error of mean sea level pressure for the control run (left panel) and for experiment ENSx2 (right panel) at 2100 UTC on 11 September 2003. The corresponding mean sea level pressure analyses at 0000 UTC 12 September are shown in Figure 7. It can be seen that the background error of the analysis-ensemble is larger than that of the control, and has a local maximum in the same location as the tropical cyclone. However, there is little difference between the analyses. The same arguments apply two days later, as shown in Figure 8 and Figure 9.

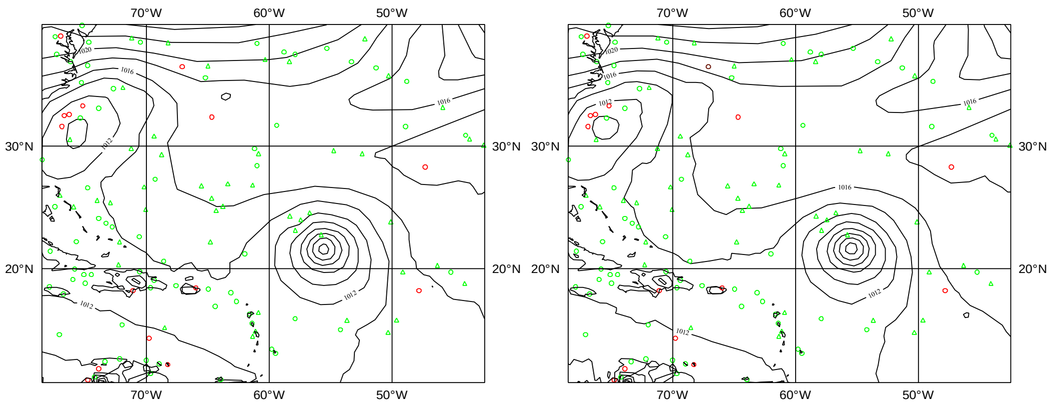

Figure 7: Analysis of sea level pressure for 12 September 2003, 0000 UTC. (a) is the control run, with background error variance calculated using the current operational method (e.g. Figure 6a). (b) used background errors from the 10-member analysis ensemble, scaled by a factor of two (e.g. Figure 6b). The contour interval is 2 hPa, with surface observation usage indicated by circles (SYNOPs and SHIPs) and triangles (DRIBUs). Green symbols denote used observations. Red symbols denote observations that were rejected by quality control. The central pressures are 1001.4 hPa and 1001.0 hPa, respectively.

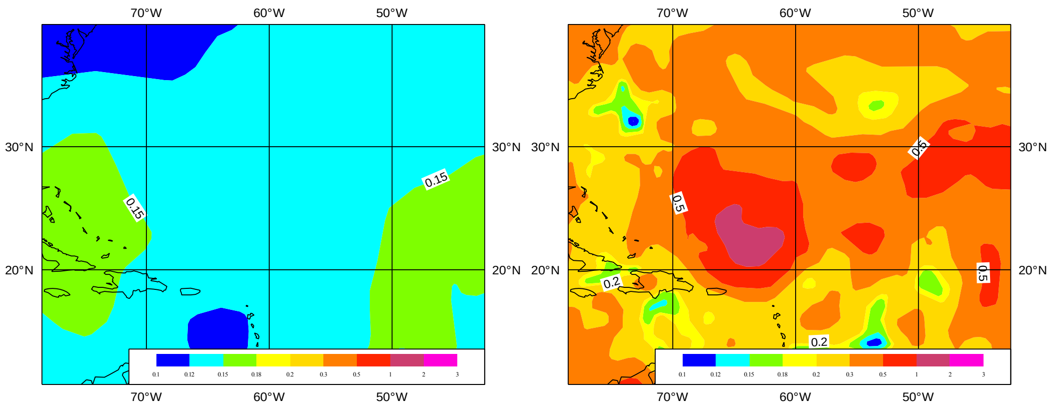

Figure 8: As Figure 6, but for 2100 UTC 13th September 2003.

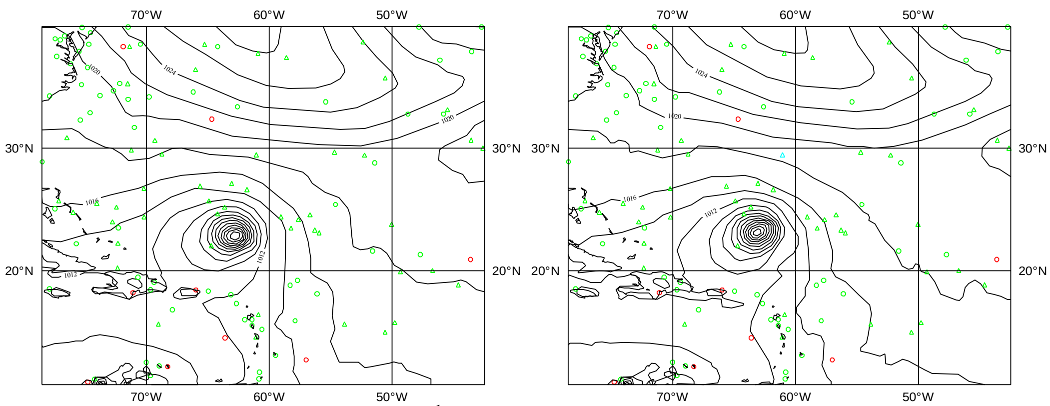

Figure 9: As Figure 7, but for 0000 UTC 14th September 2003.

A time series of the analysed central pressure of the hurricane is shown in Figure 10 For most analysis cycles, the central pressure is lower by several hPa in ENSx2 than in the control experiment. (The large discrepancy between the analysed and the observed pressure for both experiments is typical of current analysis systems, and results in part from deficiencies in resolution and from the use of background error correlations that are inappropriate to the dynamical situation. We do not address these issues in the current study).

Although background errors generated using the analysis-ensemble are larger than those of the control run for the whole period, observation usage is about the same for both experiments (not shown).

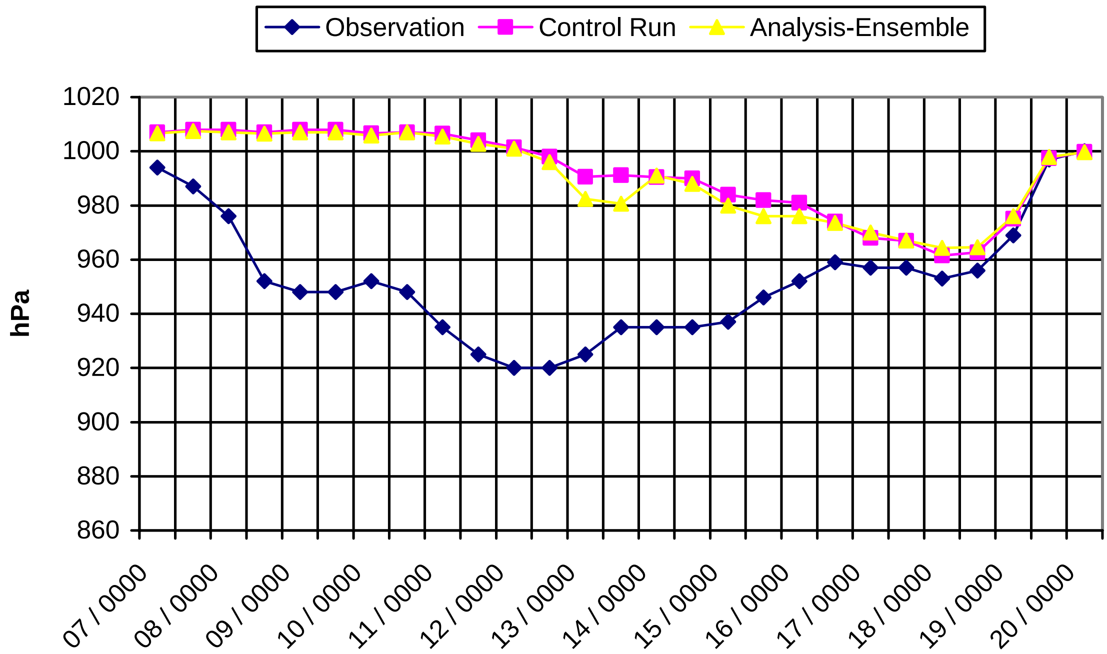

Figure 10: Time series of centre pressure of Hurricane Isabel for period 20030907 and 20030920.

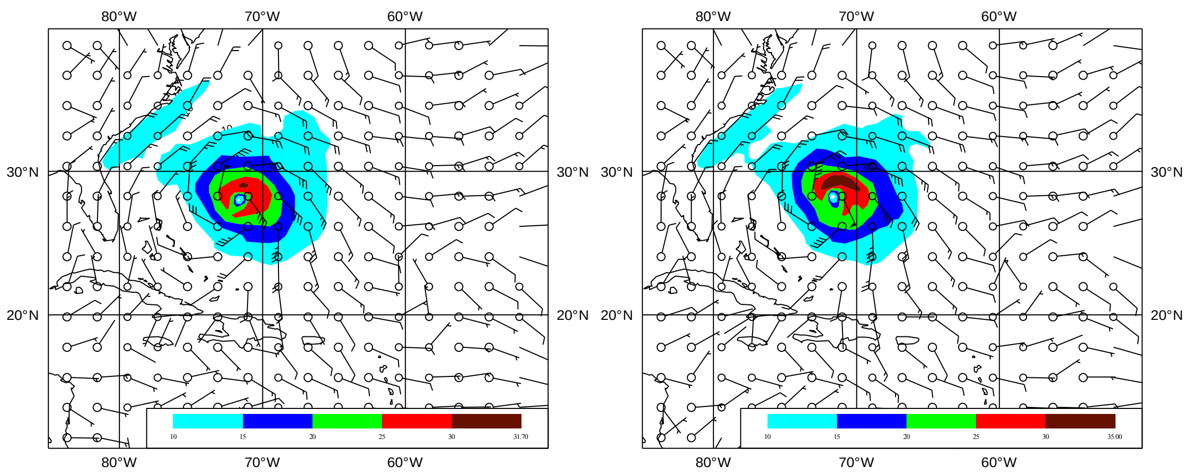

Figure 11: Analyses of 10 metre wind (m/s) at 0000 UTC on 17th September 2003, (a) is control run and (b) used background errors derived from the analysis ensemble. Wind speeds larger than 10 m/s are shaded, with a contour interval of 5 m/s (see legend).

Figure 11 shows the analysed 10m winds at 0000 UTC on 17 September. The maximum observed 10m wind speed for Hurricane Isabel was 45 m/s on 17th September. The maximum wind speed of ENSx2 was 35 m/s, whereas for the control it was 31 m/s.

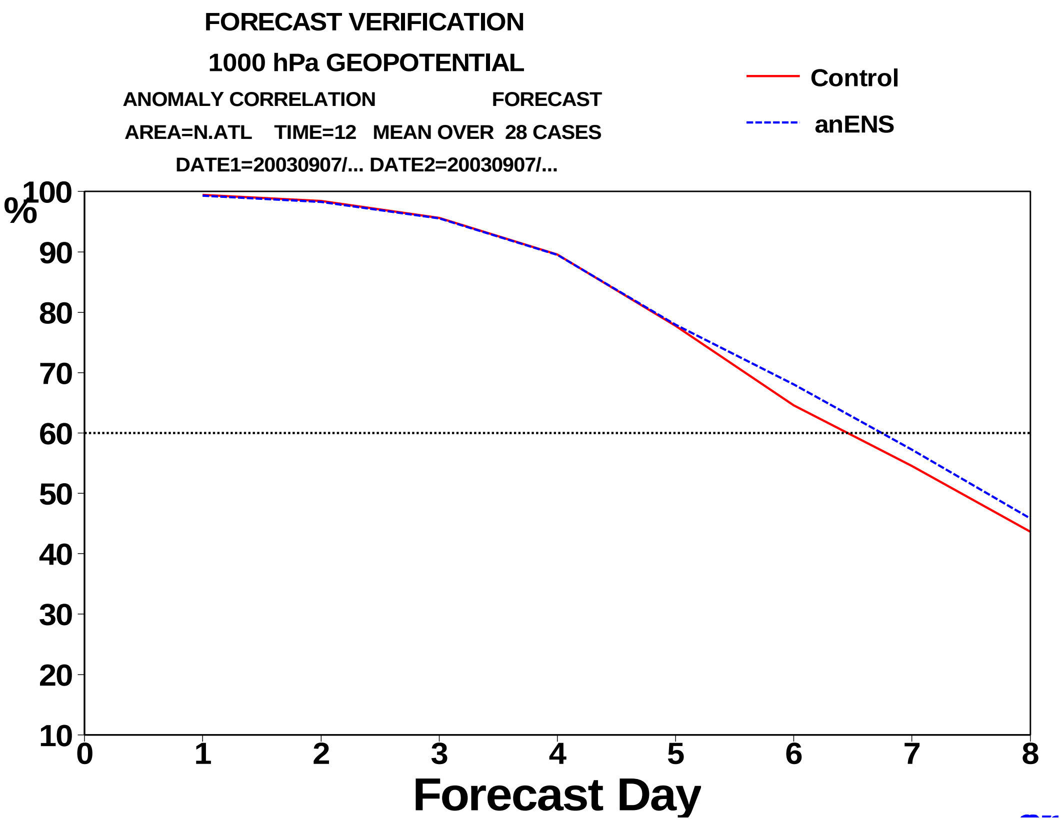

Figure 12: Forecast score for 1000 hPa Geopotential height over North Atlantic for period between 20030906 and 20031005 for the experiment (blue) which used background error derived from the 10-member analysis ensemble. The control run is shown red.

Finally, in Figure 12, we show the anomaly correlation of 1000hPa geopotential between 7 September and 5 October 2003 for the North Atlantic area. The results are close before t+120, but analysis ensemble-based forecasts are better than the control run after t+120. (It should be noted, however, that this result is unlikely to be statistically significant, given the small size of the verification area and the relatively small number of cases.)

5. Conclusions

The results given above represent a preliminary investigation into the use of background errors derived from analysis ensembles. As such, we can offer only tentative conclusions.

In the case of the second "French storm", there were significant differences between the control analysis and the analyses produced using ensemble-derived background errors. It is encouraging that use of the latter produced better analyses in this case. The other cases (the first "French storm", and hurricane Isabel) were characterized by small-scale systems that were poorly resolved by the (T511) analysis system, let alone by the (T255) ensemble members. As well as resolution, factors such as inappropriately large-scale background correlations contribute to the analysis deficiencies for small-scale tropical and mid-lattitude cyclones. It is perhaps a tall order to expect changes in the specified background error to produce improvements to the analysis without rectifying other shortcomings in the analysis formulation. Nevertheless, it is notable that for hurricane Isabel, the wind analysis in the vicinity of the cyclone was improved, and the central pressure was significantly reduced for nearly every analysis in the period 7-20 September shown in Figure 10.

Our current implementation of the analysis ensemble method underestimates the variance of background error. To compensate for the ensembles' lack of spread, we used two different approaches: constant scaling of the variances, and a hybrid approach. A constant scaling factor tuned to increase errors in dynamically active regions produced an insufficient increase of the very small spread in well-observed, dynamically inactive regions. The hybrid approach rectified this deficiency. But, neither method is satisfactory. Clearly, a better understanding of the reasons for the lack of spread of the ensemble is required.

Finally, we examined the effect of ensemble size. It seems likely that useful information about the variance of background error can be extracted from a very small (e.g. 5-member) ensemble. This suggests that for estimating background error variance, a small ensemble of fairly high resolution members may be preferable to a larger ensemble of low resolution members.

Acknowledgements

This paper summarizes the investigations conducted by the first author during his year at ECMWF as a Graduate Trainee. We wish to thank the Turkish Meteorological Service for approving his secondment, and for their financial support. We also thank colleagues in the Data Division for their valued comments.

References

Bell G.D., Halpert M.S., Schnell R.C., Higgins R.W., Lawrimore J., Kousky V.E., Tinker R., Thiaw W., Chelliah M., and Artusa A., 2000: Climate assessment for 1999. *Bull.Am.Meteor.Soc.*, **81**, 1328-1328.

Beven, J., and Cobb, H., 2004: National Hurricane Center Reports,

Buizza, R., and A. Hollingsworth, 2002: Storm prediction over Europe using the ECMWF Ensemble Prediction System. ECMWF Tech. Memo. 356, 26pp. (Available from: http://www.ecmwf.int/publications/)

Bormann N., Saarinen S., Kelly G., and Thépaut J.-N., 2003: The Spatial Structure of Observation Errors in Atmospheric Motion Vectors from Geostationary Satellite Data. *Mon.Wea.Rev.*, **131**, 706-718.

Dvorak, V., 1975: Tropical cyclone intensity analysis and forecasting from satellite imagery. *Mon.Wea.Rev.*, **103**, 420-430.

Evensen, G. 2003: The ensemble Kalman filter: theoretical formulation and practical implementation. *Ocean Dyn*. **53**, 343-367.

Fisher, M., 2003: Background error covariance modelling. pp45-64 in *Proceeding of the ECMWF Workshop on Recent Developments in Data Assimilation for Atmosphere and Ocean*, 8-12 September 2003, Reading, UK.

Fisher, M. and Courtier, P., 1995: Estimating the covariance matrices of analysis and forecast error in variational data assimilation. ECMWF Tech. Memo. 220.
(Available from: http://www.ecmwf.int/publications/)

Houtekamer, P.L. and Mitchell, H.L., 1998: :Data Assimilation Using an Ensemble Kalman Filter Technique. *Mon.Wea.Rev*., **126**: 796-811

Parrish, D.F. and Derber, J.C., 1992: National Meteorological Center's spectral statistical-interpolation analysis system. *Mon.Wea.Rev*., **120**, 1747-1763.

Savijärvi, H., 1995: Error growth in a large numerical forecast system. *Mon.Wea.Rev.*, **123**, 212-221.

Simpson, R.H. and H. Riehl (1981): *The Hurricane and Its Impact*. Louisiana State Univ. Press, Baton Rouge (IBSN 0-8071-0688-7), 398pp.

Thiebaux, J., Katz, B. and Wang, W., 2001: Mew sea-surface temperature analysis implemented at NCEP. pp159-J163 in Preprints of *18th Conf. on Weather Analysis and Forecasting*, American Meteorology Society.

Vialard, J., Vitart, F., Balmaseda, M.A., Stockdale, T.N. and Anderson, D.L.T., 2005: An Ensemble Generation Method for Seasonal Forecasting with an Ocean-Atmosphere Coupled Model. *Mon.Wea.Rev.*, **133**, 441-453.

Wernli, H., S. Dirren, M. A. Liniger, and M. Zillig, 2002: Dynamical aspects of the life-cycle of the winter storm 'Lothar' (24-26 December 1999). *Quart. J. Roy. Meteor. Soc.*, **128**, 405-430

Žagar, N., Andersson, E., Fisher, M., 2005: Balanced tropical data assimilation based on a study of equatorial waves in ECMWF short-range forecast errors, *Quart. J. Roy. Meteor. Soc*., **131**, 987-1011.